

Record of Holocene glacial oscillations in Bransfield Basin as revealed by siliceous microfossil assemblages

M. ANGELES BÁRCENA¹, RAINER GERSONDE², SANTIAGO LEDESMA¹, JOAN FABRÉS³, ANTONIO M. CALAFAT³, MIQUEL CANALS³, F. JAVIER SIERRA¹ and JOSE A. FLORES¹

¹Departamento de Geología, Facultad de Ciencias, Universidad de Salamanca, 37008 Salamanca, Spain

²Alfred Wegener Institut für Polar- und Meeresforschung, Columbusstrasse, D-27568 Bremerhaven, Germany

³GRC Geociencias Marines, Department Geologia Dinamica, Geofísica i Paleontologia, Universidad de Barcelona, Campus de Pedralbes, 08071 Barcelona, Spain

Abstract: Two gravity cores, Gebra-1 and Gebra-2 from the central and eastern basins of Bransfield Strait, West Antarctica, consist mainly of hemipelagic, laminated muds with black layers rich in sand-sized volcanic ash. Micropalaeontological (diatoms and radiolarians) and geochemical (organic and inorganic) analyses, together with radiometric dating (U/Th, ¹⁴C and ²¹⁰Pb) have been performed on both cores. AMS analyses on Total Organic Carbon yielded a ¹⁴C-age older than expected, 2810 yr BP for the core top of Gebra-1 and 2596 yr BP for Gebra-2. The downcore pattern of ages indicates a sedimentation rate of 130 cm kyr⁻¹ for Gebra-1 and 160 cm kyr⁻¹ for Gebra-2. ²¹⁰Pb anomalies suggest the core top of Gebra-1 is present-day sediment. The diatom and radiolarian assemblages are related to the sequence of neoglacial events over the last three millennia. The recent significant reduction in *Chaetoceros* resting spores is interpreted as a reduction in palaeoproductivity. The progressive increase in sea-ice taxa for the last three millennia may indicate a cooling trend. Greater sea-ice coverage during the coldest neoglacial events in the Bransfield Basin, as well as in the Weddell Sea and Bellingshausen Sea, is documented by increases in sea-ice taxa and reductions in *Thalassiosira antarctica*/*T. scotia* resting spores, *Fragilariopsis kerguelensis*, the *Lithomelissa* group and the “circumpolar” group of radiolarians. For these periods, we postulate a restricted communication between the Weddell Sea, Bellingshausen Sea and Bransfield basin. The millennial-scale changes are overprinted by a high frequency cyclicity at about 200–300 yrs, which might be related to the 200-yr solar cycle.

Received 30 December 1997, accepted 2 June 1998

Key words: Bransfield Basin, Holocene, neoglacial events, palaeoceanography, siliceous microfossils, West Antarctica

Introduction

Numerous studies on siliceous microfossils (diatoms and radiolarians) have been conducted in the Antarctic Peninsula region, including the Bransfield Basin. Since the pioneering works of Karsten (1905–07), Van Heurck (1909), and Heiden & Kolbe (1928), research in the region has primarily focused on plankton distribution (Hasle 1965, 1969, Kozlova 1966, Hargraves 1968, Fenner *et al.* 1978, Fryxell *et al.* 1988, Klöser 1990, Scharek 1991), the composition of the sea ice flora (Whitaker 1977, Krebs 1983, Gersonde 1986, Bartsch 1989), the settling assemblage (Gersonde & Wefer 1987, Abelmann & Gersonde 1991, Leventer 1991, Abelmann 1992a, 1992b) and the sedimentary record (Kellogg & Kellogg 1987, Kim & Park 1988, Zielinski 1993, Zielinski & Gersonde 1997). Although many factors may alter the composition of the original assemblage both during descent through the water column and during deposition on the seafloor, these studies have shown that siliceous microfossil assemblages can be used as a proxy indicator of palaeoceanographic conditions (sea ice extent, primary productivity, and water mass tracers).

The Holocene period has been characterized by alternating epochs of neoglacial expansion and subsequent retreat on a scale large enough to have had a significant effect on humankind (García-Cordon 1996). Following the Last Glacial Maximum (LGM) at 18 ky BP a climatic optimum was established in the Southern Hemisphere (Björck *et al.* 1996). After this climatic optimum a sequence of Holocene neoglacial episodes has been identified. One of the most significant neoglacial events is known as the Little Ice Age (Lamb 1965). The available data generally indicate a period of decreased Northern Hemisphere temperatures and stronger zonal winds between about 650 and 100 yrs ago. Data from the Southern Hemisphere concerning changes in climate over the last millennia include ice cores in the Andes (Mörner 1984), alpine glaciers in New Zealand and South America (Grove 1988), and moraines and tills on King George Island and the Antarctic Peninsula (Birkenmajer 1992). Also, evidence of these neoglacial events has been found in Antarctic marine sediments by Leventer & Dunbar (1988) and Leventer *et al.* (1996), and in Antarctic ice cores (Barnola *et al.* 1995).

The world-wide occurrence of neoglacial events indicates

a primary astronomical forcing for climatic change. Several studies have proposed a solar forcing of a 200 yr rhythm, related to reduction in sunspot activity (Wigley & Kelly 1990, Leventer *et al.* 1996). Wigley & Kelly (1990) found a strong correspondence between ^{14}C anomalies recorded in tree rings and glacier advances in both Northern and Southern Hemispheres. Also interesting is the work by Leventer *et al.* (1996) in which the authors observed that the climatic system along the Antarctic Peninsula oscillated with a 200–300 yr rhythm in the late Holocene.

The main objective of this paper is to document the variability in siliceous microfossil assemblages in Holocene sediments of the Antarctic Peninsula area, and the relationship of this variability to climatic data derived from terrestrial and marine sedimentological records. A further aim is to recognize changes in primary production, fluctuations in sea ice extent,

and surface hydrodynamics as recorded by the downcore distribution of microfossil assemblages.

Physical setting

Location, water masses and currents

The Bransfield Basin, a 100 km wide extensional basin, occupies the segment of the Antarctic Peninsula between the Hero and Shackleton fracture zones south-east of the South Shetland Islands (Fig. 1). The Bransfield Basin is a deep asymmetrical trough composed of three separate sub-basins trending SW–NE (Jeffers & Anderson 1990, Gracia *et al.* 1995, 1996). The western Bransfield Basin (WBB) lies south and west of Livingston and Deception islands, has an irregular shape and is the shallowest (<1000 m) of the three sub-basins.

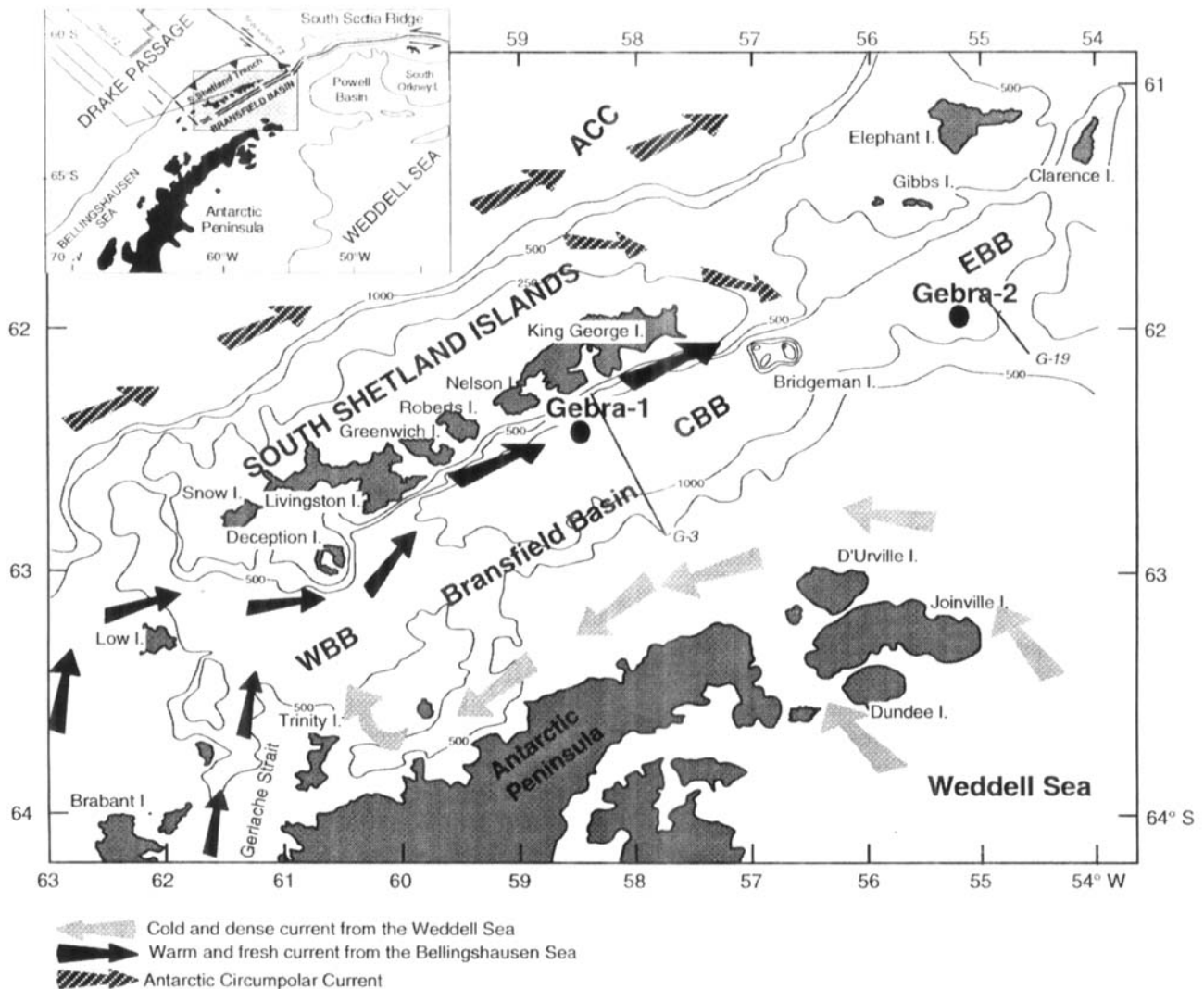


Fig 1. Core localities in the Bransfield Basin. Gebra-1 is located in the Central Bransfield Basin (CBB) and Gebra-2 in the Eastern Bransfield Basin (EBB). Arrows indicate the different surface water masses and flow directions. G-3 and G-19 lines indicate the seismic profiles in Fig. 2 (Canals *et al.* 1997).

The central Bransfield Basin (CBB) lies between Robert, Nelson and King George islands and the north-eastern tip of the Antarctic Peninsula. The CBB reaches a depth of 2000 m and features an axial, discontinuous volcanic ridge; numerous scattered volcanic cones occur on the sea floor (Gracia *et al.* 1995). The eastern Bransfield Basin (EBB) extends north-eastward, south of Elephant, Clarence and Gibbs islands, and is the deepest (2500 m) of the three sub-basins. Submarine topography of the EBB comprises several lozenge-shaped depressions separated by structural and volcanic highs (Gracia *et al.* 1996). The Deception and Bridgeman volcanic islands and highs separate the WBB from the CBB, and the CBB from the EBB, respectively (Fig. 1).

Surface waters in the Bransfield Basin have two primary sources, the Bellingshausen Sea to the west and south, and the Weddell Sea to the east (Fig. 1). Warm, relatively fresh waters flow north-eastward from the Bellingshausen Sea, enter the Bransfield Basin between Snow, Smith, and Low islands, and continue eastward, contouring Deception Island and sweeping the slope and shelf of the South Shetland Islands (Gordon & Nowlin 1978; Fig. 1). A large amount of cold dense water from the Weddell Sea enters the Bransfield Basin both south and north of Joinville and D'Urville islands, and then flows south-westward along the coast of the Antarctic Peninsula (Gordon & Nowlin 1978). The two currents meet in the vicinity of Trinity Island, where they form a front of biological significance (Amos 1987). Advection of Circumpolar Deep Water (CPDW) from Drake Passage into the Bransfield Basin is prevented by shallow sills that form the western and northern boundaries of the basin. Gordon & Nowlin (1978) have suggested that sinking surface waters form the deep and bottom waters of Bransfield Basin. These waters are characterized by their lower temperature and salinity, higher oxygen content and lower nutrient concentrations than deep waters outside the basin, although the vertical distribution of these parameters also indicates that there are significant differences within each sub-basin (Gordon & Nowlin 1978).

Present sea-ice distribution and productivity

Sea-ice distribution in Bransfield Strait follows a strong seasonal pattern. The data on annual sea-ice coverage show a maximum winter extent north to 57°S off the Antarctic Peninsula, but in summer Bransfield Strait is completely ice-free (Naval Oceanography Command Detachment 1985). Surface planktonic productivity, and therefore export production of biogenic particles to the sediments, is restricted to ice-free periods when it reaches one of the highest rates of the western Atlantic sector of the Southern Ocean (Wefer *et al.* 1988, Abelmann & Gersonde 1991). Data from sediment traps at 100 m depth yielded values of 1660 mgC m⁻² day⁻¹ for Bransfield Basin and 230 mgC m⁻² day⁻¹ in Drake Passage and northern Scotia Sea during the same period (Bodungen *et al.* 1986). As surface productivity is linked to sea ice coverage,

biogenic particle sedimentation, especially diatoms and radiolarians, is also directly related to seasonal variations in sea-ice extent. Using time-series sediment traps, Abelmann & Gersonde (1991) have shown that particle flux peaks occur during periods with open water conditions, whereas under sea ice cover the vertical flux of siliceous organisms from the surface waters is extremely low.

Sediment types and sources

Distinct sediment types occur in the Bransfield Basin as a function of bathymetry, physiography, sedimentary processes and particle sources (Ercilla *et al.* 1997, Fabres *et al.* 1997). Singer (1987), Jeffers (1988) and Jeffers & Anderson (1990) have distinguished three main sediment types. The lithofacies in shallower areas (<250 m) is represented by coarse sand and gravel. Deposits on basinward slopes, deeper than 250 m, generally comprise muddy sands and sandy muds. Sediments on the basin floor are made up of three components, in order of abundance: biosiliceous material, mostly diatoms; a terrigenous component, quartz silt; and volcanic ash.

Most of the terrigenous sediment deposited in Bransfield Basin comes from the Antarctic Peninsula margin, where thick glacio-marine progradational and aggradational units accumulated during Plio-Quaternary times (Prieto *et al.* in press a, in press b). The South Shetland Islands contribute lesser amounts of sediment. Locally, the axial volcanic lineaments form a barrier separating depositional units of South Shetland Islands and Antarctic Peninsula origins (Prieto 1996). The basin floor collects large amounts of planktonic and resuspended material. This results in high sedimentation rates for the basin floor and adjacent areas, with values ranging between 60 and 490 cm ky⁻¹ (DeMaster *et al.* 1987, Van Enst 1987, Laban & De Groot 1986, Venkatesan & Kaplan 1987, Harden *et al.* 1992, Domack *et al.* 1993, Scherer & Leventer 1995, Leventer *et al.* 1996).

Comparison of these high sedimentation rates and surface production estimates indicates that the silica accumulation rate in Bransfield Basin accounts for approximately half of the surface production rate (DeMaster *et al.* 1987). Alteration of the assemblages of siliceous organisms during vertical transport through the water column results from mechanical breakdown by grazing zooplankton and dissolution (Gersonde & Wefer 1987). Another factor affecting the composition of the biosiliceous signal in the sediment record is the input of laterally transported material (Abelmann & Gersonde 1991).

Materials and methods

Gravity cores Gebra-1 and Gebra-2 were recovered during the RV *Hesperides* cruise GEBRA-93 in the Bransfield Basin at 62°35.36'S, 58°32.53'W and 61°56.56'S, 55°10.21'W, respectively; i.e., in the central and eastern sub-basins (Fig. 1). The two cores come from sites of continuous draped sedimentation, which results in stratified seismic facies, as

observed on Bottom Parametric Source very high resolution seismic profiles (Fig. 2). Core Gebra-1 is 251 cm long and was taken south of King George Island, at 1652 m depth, below the path of the Bellingshausen Sea waters entering Bransfield Basin. Core Gebra-2, 454 cm long, comes from 1106 m depth, under the influence of both Bellingshausen Sea and Weddell Sea surface waters (Fig. 1). Both cores are dominated by biosiliceous material. They were described on board ship and sampled every 5 cm for sedimentological and geochemical analyses, and every 10 cm for micro-palaeontological studies.

Total organic carbon (TOC) and nitrogen content were determined in a Fisons model NA 1500 elemental analyser. For TOC, decalcified samples were used, while untreated samples were employed for nitrogen content determination. A modified Mortlock & Froelich (1989) extraction procedure was used to measure the biogenic silica content. This technique consists of a single alkaline extraction with 2M Na₂CO₃ over 5 hours at 85°C. The solutions obtained were analysed by ICP-AES (Inductive Coupled Plasma-Atomic Emission). The spectrometer used was a Polyscam™ G1 E (Thermo Jarrel Ash Corporation), which is a multielemental apparatus with a crossflow nebulizer and an acceleration potential of 1150 V.

Cleaning of the sediment samples and the preparation of

permanent mounts for light microscopy were done according to the settling technique described by Abelman *et al.* (in press). Absolute diatom numbers were determined from slides with randomly distributed microfossils. For counting, a Zeiss Axioplan microscope at 1000X magnification was used. A count of at least 400 diatom valves per sample was performed using the method of Schrader & Gersonde (1978). The preservation status of the fossil assemblage was estimated by visual examination. A modified Sanfilippo *et al.* (1985) technique was used to study the radiolarian component. The carbonate content as well as the organic matter were removed from the sample, which was then sieved through a 36 µm mesh. Radiolarian counts (minimum 400 individuals) were done under a Zeiss microscope at several magnifications (125X, 250X and 500X).

Age of the sediments

Only a few of the many cores recovered in Bransfield Basin contain pre-Holocene sediments (Singer 1987, Harden *et al.* 1992). Since the widely recognised pre-Holocene diatom marker species *Eucampia antarctica* (Castr.) Mang. (Burckle & Cooke 1983, Burckle 1984, Burckle & Burak 1988) was not found in the two Gebra cores, they are likely to be younger

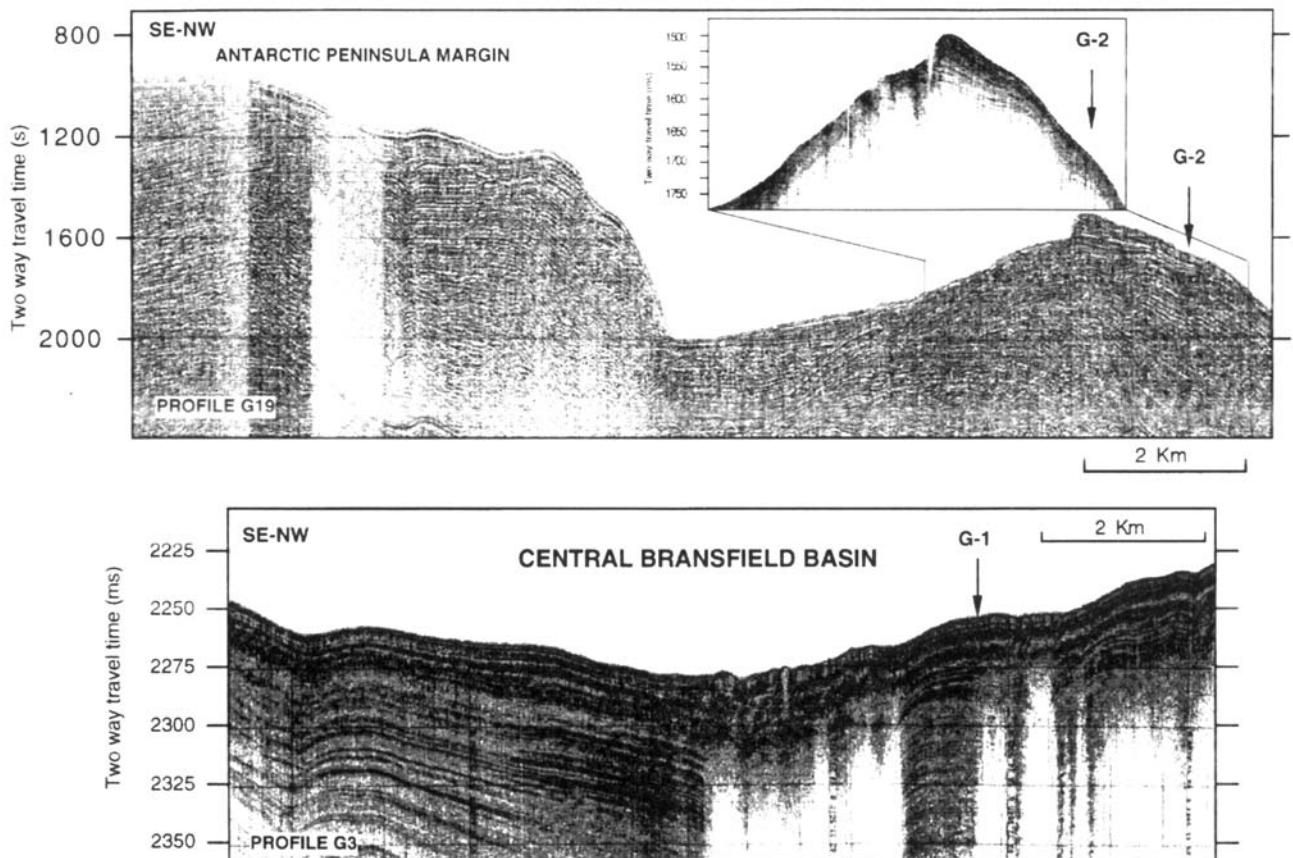


Fig 2. Seismic profiles G-3 and G-19 (Bottom Parametric Source very high resolution profiles), from the CBB and EBB. Location of core sites is indicated by arrows.

than 18 ka. Three different radiometric techniques, $^{230}\text{Th}/^{234}\text{U}$ and AMS ^{14}C chronology and ^{210}Pb excess, have been used to determine the age and sedimentation rates of the cores.

$^{230}\text{Th}/^{234}\text{U}$ radioactivity, analysed in core Gebra-2, was quite stable along the core, indicating a sedimentation rate higher than 80 cm kyr^{-1} . Three levels in each core were sampled for AMS ^{14}C dating on Total Organic Carbon (Table I, Fig. 3). The near-surface ages were older than expected, $2796 \pm 34\text{ yr BP}$ for the sample at 25 cm in core Gebra-2 and $2985 \pm 39\text{ yr BP}$ for the sample at 28 cm in core Gebra-1. Despite this, the ages display a clear downcore pattern indicating a linear sedimentation rate of 160 cm kyr^{-1} for Gebra-2 and 130 cm kyr^{-1} for Gebra-1, in agreement with the accumulation rates given in the literature (Fig. 3a & b). The accumulation rate is higher in core Gebra-2, under the influence of the higher productivity of the cold Weddell Sea water.

Core top ages extrapolated from linear sedimentation rates are 2810 yrs for Gebra-1 and 2596 for Gebra-2. These are of the same order of magnitude as those obtained by Harden *et al.* (1992), Domack *et al.* (1993) and Leventer *et al.* (1996) in the Antarctic Peninsula region. Radiocarbon dating of Antarctic sea water samples and marine organisms has yielded anomalously old ages of up to 2860 yrs (Stuiver *et al.* 1981). Two main effects have been considered to explain the high age of the sediments: the large and regionally variable reservoir effect of 1200–1400 yrs (Stuiver *et al.* 1981, Berkman *et al.* 1998, Ingólfsson *et al.* 1998) and possible inputs of older eroded sediment, transported by currents or by ice rafting. The input of terrestrial organic matter is considered insignificant, since most of the organic matter present in the sediments is derived from primary local producers (Venkatesan & Kaplan 1987).

^{210}Pb was determined by γ -spectrometry in an n-type high purity germanium detector (courtesy of Dr B. Quintana, University of Salamanca). Preliminary data indicate an

Table I. ^{14}C conventional ages of the three samples from each core.

Core	Depth (cm)	^{14}C conventional age (yrs)
Gebra-1	28–29	2585 ± 39
	135–136	3959 ± 47
	240–241	4646 ± 37
Gebra-2	25–26	2796 ± 34
	225–226	3916 ± 36
	440–441	5385 ± 39

excess ^{210}Pb activity in the first 10 cm of core Gebra-1, while in the first 10 cm of Gebra-2 ^{210}Pb is in equilibrium with other radionuclides. These preliminary data allow us to interpret the core top of Gebra-1 as belonging to the last sixty years, while Gebra-2 could be somewhat older. Therefore, we consider that at least 50 cm of Gebra-2 (corresponding to the industrial period of human activity) could have been lost during the coring process.

Results

Diatoms

High numbers of diatom valves per gram of dry sediment were observed in both cores, ranging from 1×10^8 – 35×10^8 . Diatom assemblages are dominated by *Chaetoceros* resting spores (RS, 65–90% of the total). The rest of the assemblage includes taxa such as *Fragilariopsis curta* (V. Heur) Hasle, *F. cylindrus* (Grun.) Hasle, *F. obliquecostata* (V. Heur) Hasle, *F. sublinearis* (V. Heur) Hasle and *F. vanheurckii* Hasle. These species have been grouped as sea-ice taxa since all of them live in the sea ice and/or sea-ice related environments (Gersonde 1986, Zielinski & Gersonde 1997). Another interesting component of the diatom assemblage is *Thalassiosira antarctica* Comber/*T. scotia* Fryxell and Hoban in the resting spore stage (RS). These species are open-ocean

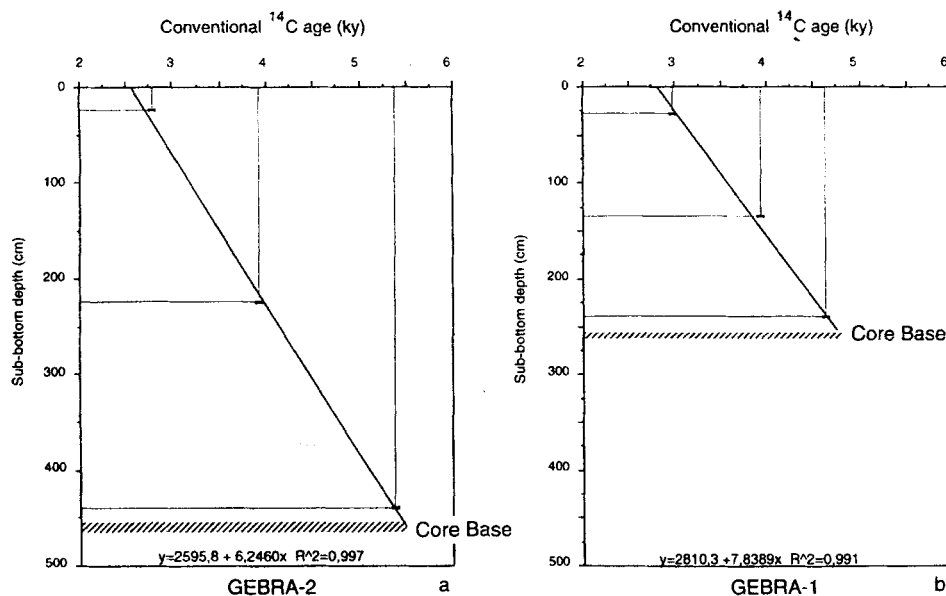


Fig 3. a. Age-depth curve for core Gebra-2. b. Age-depth curve for core Gebra-1. See also Table I.

forms which are more abundant in the Weddell and Scotia Seas than in the Bransfield Basin area; their occurrence in the Bransfield Basin has been related to incursions of cold Weddell Sea surface waters into the area (Abelmann & Gersonde, 1991). Species such as *Fragilariopsis kerguelensis* (O'Mea.) Hasle, *Rhizosolenia* spp., *Proboscia alata* (Brightwell) Sundstrom, *Thalassiosira gracilis* (Karsten) Hustedt, *T. gravida* Cleve, *T. oliverana* (O'Mea.) Sour., *T. trifurcata* Fryxell, *T. tumida* (Jan.) Hasle, etc. are also common components of the fossil diatom assemblage. Tables II & III give the absolute and relative abundances. The species distribution in both cores as well as their relative abundance are in agreement with the values in the literature for the Bransfield Basin area (Gersonde & Wefer 1987, Wefer *et al.* 1988, 1990, Abelmann & Gersonde 1991, Leventer 1991, Zielinski 1993, Zielinski & Gersonde 1997).

Diatom abundance data are shown in Fig. 4. The large numbers of *Chaetoceros* RS in the sediments tend to mask the signal of the rest of the assemblage. In general, the abundance of *Chaetoceros* RS in core Gebra-2 tends to decrease toward the top. Maximum values occur in the lower part, with lower values from 265 to 185 cm and a minimum at the top. In Gebra-1 there is an irregular decrease in abundance from 100 cm to the core-top. The abundance pattern of the sea-ice

Table II. Abundance of the most significant diatom groups in core Gebra-1.

Depth valves (cm)	<i>Ch</i> /g dry sed (x10 ⁸)	Sea-ice taxa %	<i>F.ker</i> RS%	<i>T.ant</i> / <i>T.sco</i> %	<i>Rh</i> spp. %	Oth %	
1	0.33	74.34	6.95	0.96	10.1	1.20	6.47
11	0.47	74.85	11.4	2.99	3.89	1.20	5.69
21	1.39	92.86	2.60	0.65	1.30	0.43	2.16
31	1.19	78.04	5.84	2.80	4.44	3.50	5.37
41	0.76	81.37	7.28	2.36	4.07	1.28	3.64
51	2.34	84.04	5.49	1.50	4.24	1.25	3.49
61	3.65	90.04	7.37	0.40	0.80	0.20	1.20
71	0.82	77.42	7.96	2.37	4.95	2.58	4.73
81	1.23	82.77	7.58	1.33	3.03	0.57	4.73
91	1.42	90.77	4.05	0.90	1.13	0.23	2.93
101	1.12	91.87	3.77	0.40	0.99	0.20	2.78
111	0.77	89.31	3.09	1.90	0.95	1.19	3.56
121	0.70	85.22	7.92	0.79	2.64	0.26	3.17
131	0.61	80.50	4.13	2.98	5.50	0.46	6.42
141	3.23	91.44	3.15	0.68	0.68	0.23	3.83
151	0.82	81.36	6.82	2.05	4.09	0.91	4.77
161	1.26	82.56	5.52	1.55	4.86	0.88	4.64
171	2.08	87.06	4.00	2.12	1.18	3.06	2.59
181	0.77	88.20	3.22	0.64	4.94	0.86	2.15
191	1.06	81.58	3.59	2.63	5.02	1.44	5.74
201	0.68	77.94	4.58	2.29	4.87	2.58	7.74
211	0.65	78.62	5.41	2.46	3.93	3.93	5.65
221	1.92	89.65	3.93	0.83	1.04	2.48	2.07
231	0.88	85.32	3.98	1.00	2.49	4.98	2.24
241	0.78	85.75	2.85	0.52	4.66	3.11	3.11
251	0.43	91.19	4.76	0.24	0.95	1.19	1.67

Ch = *Chaetoceros*; *F.ker* = *Fragilariopsis kerguelensis*; *T.ant*/*T.sco* = *Thalassiosira antarctica*/*T. scotica*; *Rh* = *Rhizosolenia*; Oth = others.

group reflects the opposite behaviour to that observed in *Chaetoceros* RS. In both cores, sea-ice taxa increase from the base to the top, reaching maximum values at 10–20 cm, but with subsidiary maxima and minima (Fig. 4).

Table III. Abundance of the most significant diatom groups in core Gebra-2

Depth valves (cm)	<i>Ch</i> /g dry sed (x10 ⁸)	Sea-ice taxa %	<i>F.ker</i> RS%	<i>T.ant</i> / <i>T.sco</i> %	<i>Rh</i> spp. %	Oth %	
1	0.94	65.01	6.71	4.66	7.87	2.33	13.4
10	2.93	72.96	11.8	3.00	2.15	1.72	8.37
20	2.84	80.00	8.33	2.92	3.33	0.21	5.21
30	3.22	79.82	8.97	1.79	3.14	3.14	3.14
40	2.87	76.04	8.54	1.88	2.92	3.96	6.67
45	3.75	79.68	7.45	1.81	4.29	2.03	4.74
50	4.13	89.69	3.81	1.35	1.35	1.79	2.02
60	2.16	78.02	8.41	2.80	1.72	1.29	7.76
70	4.07	84.78	6.34	1.69	1.27	1.27	4.65
75	4.67	83.00	6.71	2.46	0.89	3.36	3.58
80	2.57	82.23	7.29	0.91	2.28	2.05	5.24
85	2.69	83.90	7.84	2.12	2.75	0.21	3.18
95	6.30	79.96	7.13	1.78	2.67	2.67	5.79
100	7.04	87.34	5.87	0.73	1.10	0.92	4.04
110	5.13	84.21	8.37	0.72	2.87	0.48	3.35
120	1.84	85.39	4.94	1.35	2.25	1.80	4.27
130	5.02	83.64	8.41	1.59	2.27	0.23	3.86
135	5.14	88.00	5.33	1.56	2.00	1.56	1.56
140	3.16	86.61	5.18	1.94	1.51	1.51	3.24
150	5.53	85.33	5.79	1.35	1.16	2.12	4.25
160	1.90	78.86	7.60	1.90	2.38	2.38	6.89
170	5.58	89.33	3.75	0.56	1.12	1.12	4.12
180	2.93	86.61	4.60	0.84	1.67	1.26	5.02
190	4.25	84.26	5.18	1.99	1.59	1.59	5.38
200	1.82	72.50	8.41	3.64	5.00	4.32	6.14
210	6.08	85.09	4.97	2.69	2.28	1.45	3.52
220	2.15	79.96	4.64	0.84	4.22	5.06	5.27
230	5.66	83.04	5.01	1.73	2.50	1.54	6.17
240	2.53	76.89	7.34	1.51	3.46	4.54	6.26
250	5.67	76.70	10.3	1.03	2.47	2.89	6.60
260	2.53	81.18	5.34	1.97	1.97	3.37	6.18
270	6.73	85.03	7.10	1.92	1.92	0.19	3.84
280	5.60	84.40	5.56	1.71	1.92	0.85	5.56
290	3.79	83.00	4.66	2.23	2.02	2.83	5.26
300	9.10	88.59	6.22	0.62	0.00	1.66	2.90
310	5.29	81.67	6.03	1.62	1.39	3.48	5.80
320	3.44	87.97	6.02	0.50	2.26	1.00	2.26
330	4.94	87.70	5.61	1.08	1.08	1.63	2.89
340	5.03	84.19	5.54	1.23	1.85	2.67	4.52
350	3.95	85.45	3.84	2.02	3.43	2.02	3.23
360	4.03	87.61	4.65	0.44	1.55	3.32	2.43
370	3.55	84.37	5.78	1.07	3.21	2.36	3.21
380	3.32	88.86	4.55	0.91	1.82	1.14	2.73
390	4.09	88.91	3.70	0.92	3.70	0.46	2.31
400	0.86	86.78	3.31	0.55	3.86	1.10	4.41
410	5.09	87.21	4.58	0.38	1.91	2.48	3.44
420	1.96	82.77	5.67	2.10	4.62	2.10	2.73
430	3.99	87.37	4.71	1.50	2.57	1.07	2.78
440	3.39	84.06	5.80	1.93	2.90	0.48	4.83
445	2.82	89.01	4.02	1.34	2.14	0.80	2.68

Ch = *Chaetoceros*; *F.ker* = *Fragilariopsis kerguelensis*; *T.ant*/*T.sco* = *Thalassiosira antarctica*/*T. scotica*; *Rh* = *Rhizosolenia*; Oth = others.

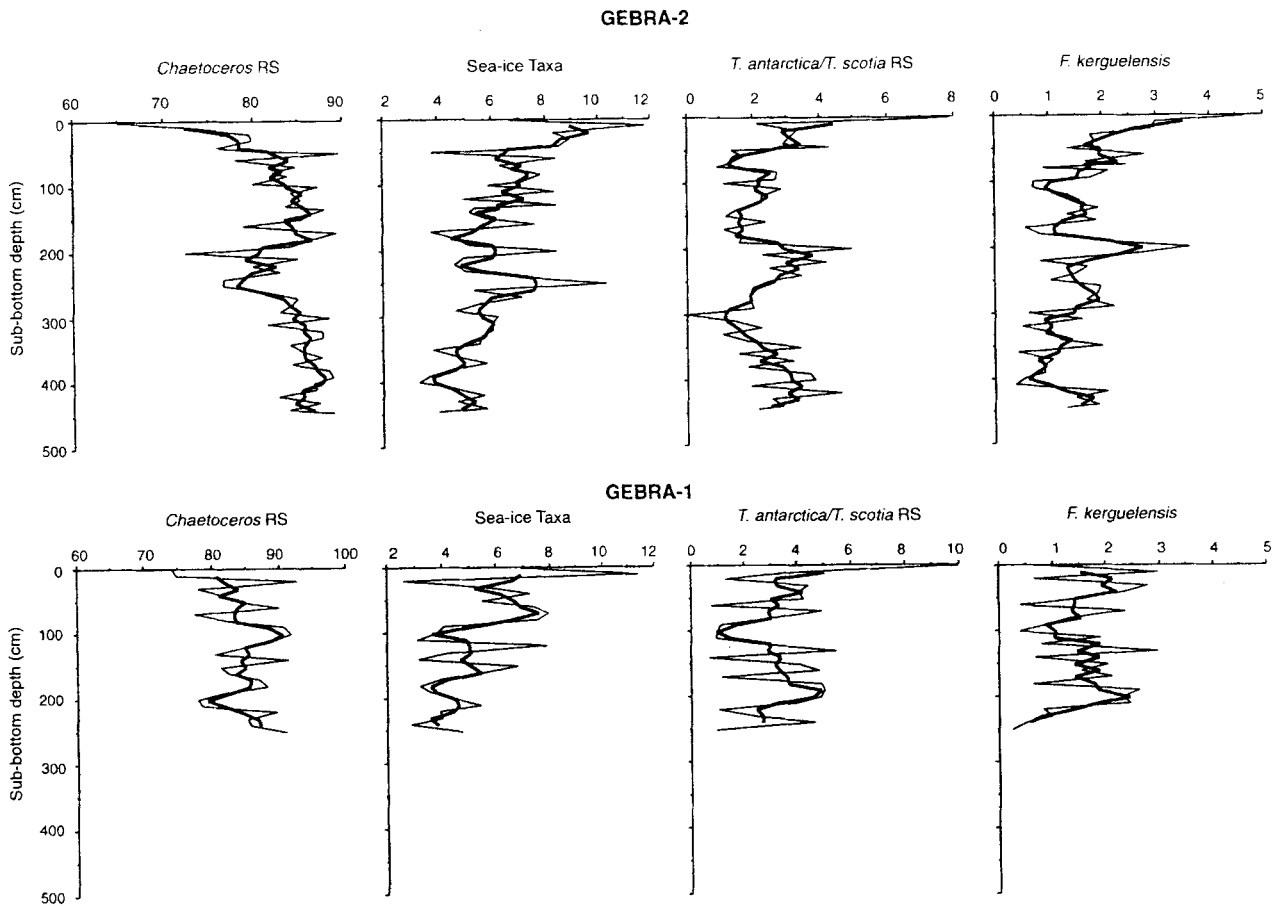


Fig 4. Diatom abundance (% of the assemblage) in Gebra-2 and Gebra-1. Thicker line indicates a three-point smoothing.

In Gebra-2, *T. antarctica/T. scotia* resting spores show an inverse relationship to the *Chaetoceros* RS abundance curve and have a quasicyclic downcore distribution. Three maxima are observed: from the core base to 350 cm, between 240 and 190 cm, and from 50 cm to the core top. *Thalassiosira antarctica/T. scotia* RS and the sea-ice taxa group seem to be inversely correlated in the lower part of the core, from the base to 320 cm, while both curves seem to covary from 190 cm to the top. In core Gebra-1, *T. antarctica/T. scotia* RS show two maxima in abundance at approximately 205–180 cm and at the core top respectively (Fig. 4).

Fragilariopsis kerguelensis is less abundant than *T. antarctica/T. scotia* RS. In both cores, its abundance changes are parallel to, but quantitatively less important than, those found for *T. antarctica/T. scotia* RS. The highest abundances in both cores are only 3.5% of the entire assemblage (Fig. 4), approaching the error margins of the counting method. Other authors have found that this taxon accounts for less than 2.5% of the diatom assemblage from Bransfield Basin (Gersonde & Wefer 1987, Leventer 1991, Abelmann & Gersonde 1991).

Radiolarians

Values of radiolarians per gram of dry sediment range between 5×10^3 and 23×10^3 . More than 40 radiolarian taxa were identified. While typical circumpolar species such as *Cycladophora davisiana* Ehrenberg or the *Antarctissa denticulata* (Ehrenberg) Petrushevskaya /*strelkovi* Petrushevskaya group are rare in both cores, 80% of the total radiolarian assemblages is composed of three species that have a bipolar distribution; *Plectacantha oikiskos* (Jorgensen), *Phormacantha hystrix* (Jorgensen) and *Lithomelissa setosa* (Jorgensen). The known distribution of these three species with respect to the water masses allowed us to classify them within two ecological groups; the *Phormacantha/Plectacantha* group and the *Lithomelissa* group. Radiolarian abundance data are given in Fig. 5 and Tables IV & V.

The *Phormacantha/Plectacantha* group has been considered as a coastal indicator (Abelmann 1992a). In cores Gebra-1 and Gebra-2 it constitutes 40–70% of the total assemblage. The *Lithomelissa* group accounts for 15–40%. The *Lithomelissa* group has been related to pelagic conditions since species of the genus *Lithomelissa* are associated with the colder water from the Weddell Sea (Abelmann 1992a, 1992b).

The general trend of the *Lithomelissa* group in Gebra-2 is to decrease towards the top of the core. Maximum values occur below 382 cm. Two minima were recorded, from 302 cm to 262 cm and from 112 cm to 82 cm (Fig. 5). The *Phormacantha/Plectacantha* group abundance is inversely correlated with the *Lithomelissa* group. The abundance patterns of the *Lithomelissa* group and the *Phormacantha/Plectacantha* group in core Gebra-1 are cyclic and inversely correlated (Fig. 5).

Typical circumpolar species such as *Antarctissa denticulata* and *A. strelkovi* are rare in both cores, where the genus *Antarctissa* accounts for less than 3% of the entire assemblage. *Larcopyle buetschlii* Dreyer, which is related to warmer waters (Molina-Cruz 1977), also has low values (below 5% of the entire assemblage). These species have been considered as the "circumpolar group" since all of them prefer warmer or circumpolar waters (Tables IV & V, Fig. 5).

Organic carbon, nitrogen and biogenic opal

The mean TOC content is 1.19% for Gebra-1 and 1.15% for Gebra-2 (Fig. 6). The mean nitrogen content is almost the same for both cores: 0.18% in Gebra-1 and 0.19% in Gebra-2. In contrast, the mean biogenic opal content is higher in Gebra-2 (22.63%) than in Gebra-1 (16.73%).

The overall patterns of the three organic components are

very well correlated, and the most striking features are recorded by all three components (Tables VI & VII, Fig. 6). The main features of Gebra-1 are an increase in TOC, N and biogenic silica from the base of the core to 200 cm, a gradual but irregular decrease up to 120 cm, then three well-defined peaks at 90, 50 and 30 cm. Gebra-2 has variable values of TOC, N and biogenic silica from the base of the core up to a minimum at 300 cm, and a broad peak followed by a minimum at 180 cm. The uppermost 120 cm displays a series of more or less symmetrical cycles with a thickness of 20–30 cm. The peak in biogenic silica at 365 cm is a diatom ooze layer. Yoon *et al.* (1994) observed a similar diatom ooze in several gravity cores from the CBB, which they used to correlate the cores.

Discussion

We have constructed an age model for the two cores based on a combination of radiocarbon ages, ^{210}Pb determination and microfossil evidence. The ^{14}C ages given for both cores are in agreement with other cores recovered in the studied area. The ^{210}Pb analyses indicate the core top of Gebra-1 is recent, while the core top of Gebra-2 is at least 150 yrs older. Gebra-2 also shows an exceptionally high amount of sea-ice taxa at the core top (around 10%; Fig. 7), which is not in agreement with current climatic conditions, but rather with colder conditions. The age model, in calendar years, is given in Fig. 7; note that

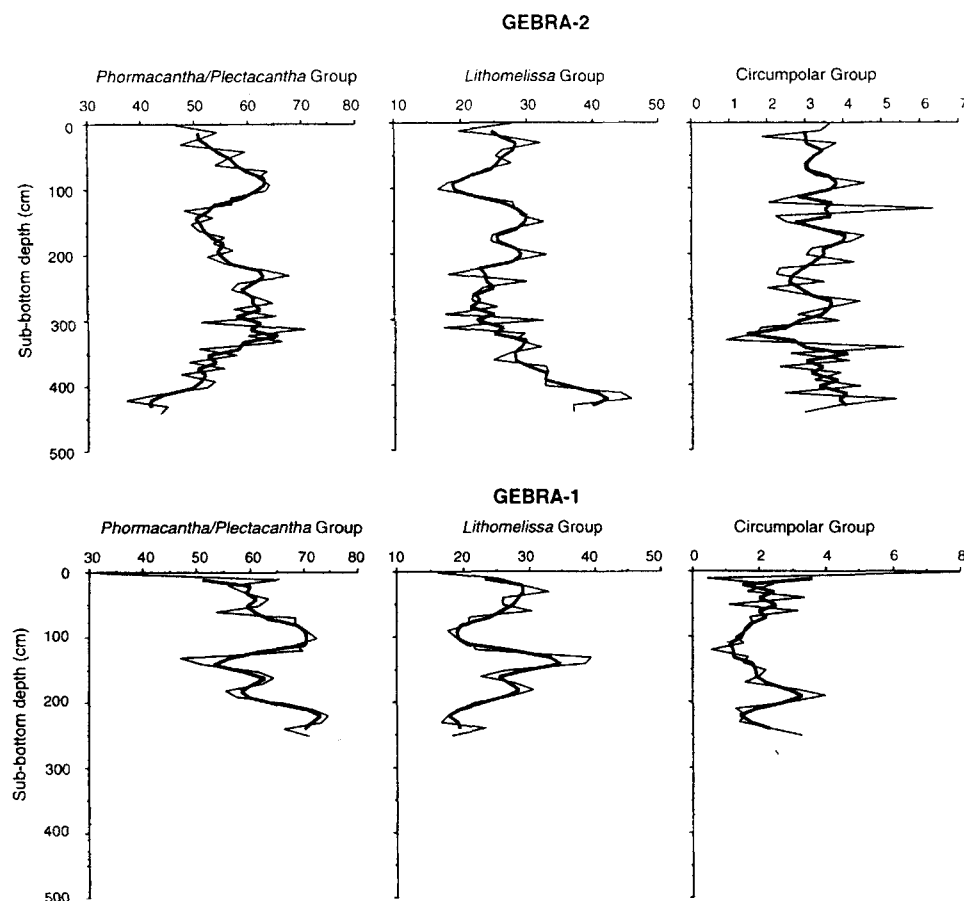


Fig 5. Radiolarian abundance (% of the assemblage) in Gebra-2 and Gebra-1. Thicker line indicates a three-point smoothing.

Table IV. Abundance of the most significant radiolarian groups in core Gebra-1.

Depth (cm)	Rads/gr dry (x10 ³)	<i>Phorm./Plect.</i> Group%	<i>Lithomelissa</i> spp%	Circumpolar Group%
1	0.81	32.00	16.00	8.00
11	6.89	65.56	25.31	0.41
21	7.95	55.96	28.44	2.45
31	19.53	59.22	32.95	1.61
41	10.21	63.51	26.01	3.38
51	14.80	61.57	25.98	1.07
61	9.64	53.66	30.49	3.17
71	15.70	68.48	20.63	1.72
81	17.44	68.26	20.65	1.81
91	6.91	70.68	17.59	1.63
101	8.73	72.42	18.82	1.29
111	7.32	68.77	21.07	1.53
121	4.85	69.84	21.69	0.53
131	5.47	46.91	39.51	1.65
141	15.84	51.14	38.64	1.51
151	9.00	61.60	26.24	2.21
161	20.25	64.44	22.44	2.00
171	15.48	62.40	27.52	1.55
181	9.36	55.29	30.53	3.12
191	14.58	57.41	27.47	4.01
201	20.70	66.74	21.52	2.83
211	9.00	71.75	19.00	1.25
221	14.35	74.61	17.56	1.57
231	19.39	73.32	16.47	1.39
241	13.90	66.34	23.30	2.27
251	9.58	70.89	18.08	3.29

Table V. Abundance of the most significant radiolarian groups in core Gebra-2

Depth (cm)	Rads/gr dry (x10 ³)	<i>Phorm./Plect.</i> Group%	<i>Lithomelissa</i> spp%	Circumpolar Group%
2	8.82	46.55	27.80	3.66
12	11.15	54.17	19.42	3.41
22	12.76	51.06	26.52	1.83
32	13.08	47.25	32.11	3.82
42	16.80	59.52	26.31	3.45
52	13.61	56.35	25.13	3.17
62	11.31	53.93	27.60	2.97
72	22.94	63.65	23.60	3.01
82	15.37	61.83	22.01	3.28
92	16.57	63.99	17.89	4.59
102	21.00	63.36	16.48	3.68
112	9.18	56.67	22.55	2.74
122	10.71	56.97	27.73	2.02
132	6.82	48.02	28.23	6.33
142	18.02	53.50	29.08	2.22
152	19.17	49.33	32.63	2.49
162	11.66	50.92	27.45	3.49
172	14.98	55.62	24.74	4.54
182	11.37	53.45	24.38	4.19
192	12.03	57.35	27.80	3.16
202	14.04	52.34	32.94	3.04
212	16.83	55.76	27.09	4.29
222	13.44	63.11	23.20	2.32
232	11.34	67.77	17.99	2.25
242	11.05	57.96	29.94	3.50
252	11.96	56.86	23.41	2.01
262	11.75	61.41	21.75	3.06
272	9.29	64.54	21.51	4.46
282	19.85	57.22	25.45	3.64
292	8.66	65.06	17.47	2.79
302	5.40	51.06	32.40	3.87
312	18.18	70.69	17.23	1.78
322	19.62	59.82	29.54	1.65
332	12.04	66.31	28.08	0.86
342	14.08	50.72	32.13	5.56
352	11.83	57.76	27.30	2.59
362	9.58	48.87	24.81	4.14
372	9.62	55.30	32.69	2.30
382	9.62	47.27	33.20	3.91
392	13.43	53.60	32.53	3.20
402	11.63	52.22	32.60	4.43
412	11.74	42.88	44.34	2.43
422	11.41	37.22	45.74	5.36
432	8.91	44.85	36.97	3.84
442	13.43	43.57	37.00	2.95

the absence of a precise reservoir correction for the ¹⁴C ages could induce some errors in dates.

Wigley & Kelly (1990) recognised six cold periods in the last three millennia, based on glacier advances and retreats as well as on ¹⁴C anomalies in tree-rings (Fig. 7). Those periods have been interpreted as neoglacial events similar to the Little Ice Age. Leventer *et al.* (1996) related variations in magnetic susceptibility in cores to climatic cooling events during the Holocene, and considered that those colder events could correspond to minimum sun spot activity. The variations in the siliceous microfossil abundance patterns of Gebra-1 and Gebra-2 seem to be closely related to Holocene neoglacial global events. Figure 7 shows the relationship between those events and the abundance pattern of *Chaetoceros* RS and sea-ice taxa. Higher values of sea-ice taxa are in phase with glacial advances characterized by minimum values in *Chaetoceros* RS. The calendar years given in this paper are subject to considerable uncertainty, but we have tentatively identified six cold periods in core Gebra-2, and four in Gebra-1 (Fig. 7). Therefore, changes in species composition reflect changes in environmental conditions, e.g. water masses and sea-ice coverage.

Significance of diatoms in Bransfield Basin

Chaetoceros RS may be well preserved in sediments; resting spores are capable of surviving for lengthy periods under

adverse conditions (low nutrients, low light, etc.), and their formation is thought to be induced by stress in environmental conditions: low light intensity (Klöser 1990), nutrient depletion (Leventer 1991) or stable water masses (Leventer *et al.* 1996). The formation of resting spores is mainly associated with neritic environments and their massive production is related to the latest stages of diatom blooms (Leventer 1991). Massive sedimentation of *Chaetoceros* RS may control the high accumulation rates of biogenic silica in Antarctic sediments (DeMaster *et al.* 1987, Bareille *et al.* 1991); thus, high concentrations of *Chaetoceros* RS in the Bransfield Basin

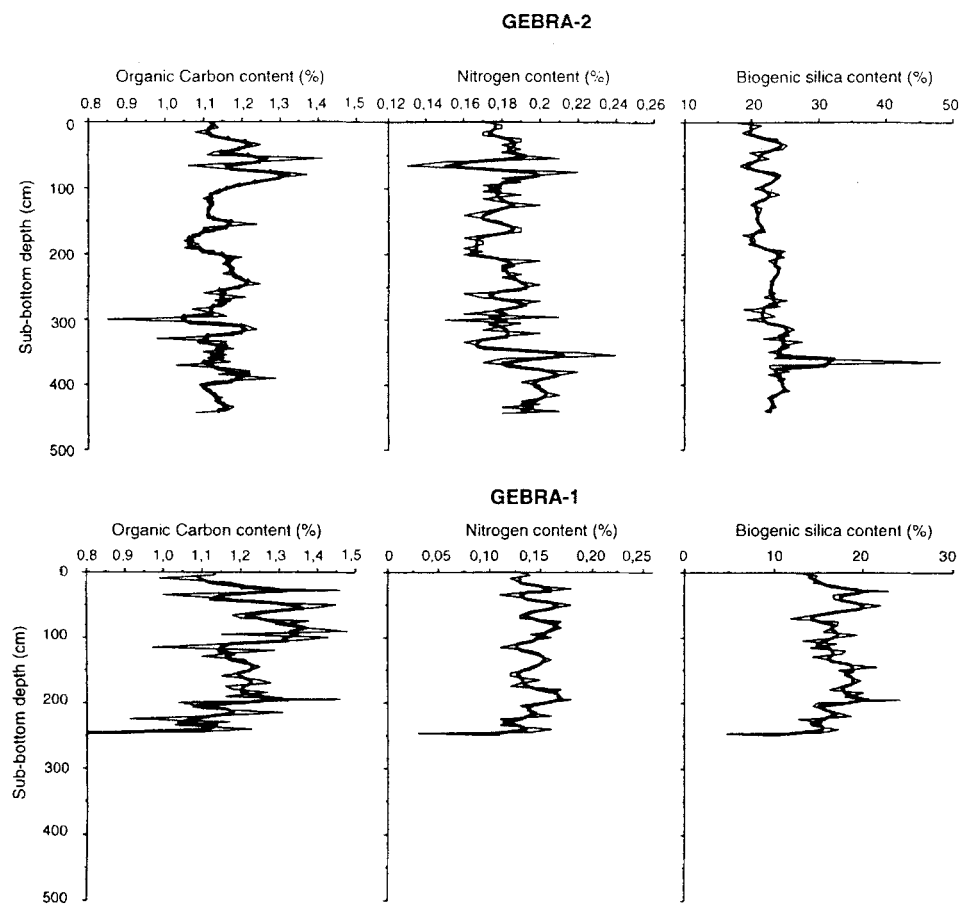


Fig 6. Total organic carbon, nitrogen and biogenic silica values obtained from cores Gebra-1 and Gebra-2. Thicker line indicates a two points smoothing.

Table VI. The total organic carbon (TOC), nitrogen, and biogenic silica content in Gebra-1.

Depth (cm)	TOC%	Nitrogen %	Biogenic % silica	Depth (cm)	TOC%	Nitrogen %	Biogenic % silica
0	1.14	0.13	12.20	130	1.10	0.15	14.29
5	1.13	0.14	14.85	135	1.21	0.16	16.62
10	0.99	0.12	14.55	140	1.22	0.15	17.82
15	1.17	0.13	14.39	145	1.25	0.14	21.59
20	1.21	0.14	17.29	150	1.23	0.14	17.23
25	1.20	0.18	17.80	155	1.20	0.12	18.49
28	1.46	0.16	22.93	160	1.15	0.12	18.14
30	1.30	0.14	19.48	165	1.25	0.15	19.76
35	1.00	0.11	16.54	170	1.28	0.13	18.96
40	1.17	0.14	16.83	175	1.16	0.12	17.63
45	1.19	0.16	18.98	180	1.18	0.17	16.19
50	1.45	0.18	22.00	185	1.27	0.16	20.12
55	1.39	0.16	19.69	190	1.16	0.17	17.94
60	1.26	0.14	17.19	195	1.36	0.17	20.50
65	1.18	0.13	14.00	196	1.46	0.18	24.11
70	1.20	0.13	11.83	200	1.04	0.15	14.90
75	1.38	0.17	17.27	205	1.09	0.13	14.46
80	1.29	0.16	17.10	210	1.10	0.14	15.50
85	1.35	0.17	16.47	215	1.31	0.14	17.38
90	1.48	0.16	15.56	220	1.14	0.16	18.69
95	1.15	0.14	19.36	225	0.91	0.11	12.71
100	1.43	0.16	16.73	230	1.17	0.12	15.45
105	1.35	0.14	13.24	235	1.03	0.11	14.16
110	1.19	0.13	17.03	240	1.23	0.16	17.25
115	0.97	0.11	14.13	245	1.08	0.14	15.30
120	1.29	0.14	18.01	247	0.26	0.03	4.69
125	1.17	0.15	17.65	250	0.72	0.11	10.70

Table VII. The total organic carbon (TOC), nitrogen, and biogenic silica content in Gebra-2.

Depth (cm)	TOC %	Nitrogen %	Biogenic % silica	Depth (cm)	TOC %	Nitrogen %	Biogenic % silica
0	1.11	0.17	17.58	225	1.18	0.18	24.06
5	1.13	0.18	21.49	230	1.15	0.19	23.81
10	1.14	0.18	20.21	235	1.20	0.18	23.68
15	1.08	0.17	18.61	240	1.20	0.19	22.56
20	1.12	0.17	19.97	245	1.25	0.20	23.18
25	1.16	0.19	23.81	250	1.18	0.19	22.96
30	1.21	0.19	23.81	255	1.15	0.19	22.44
35	1.25	0.18	25.32	260	1.10	0.16	23.58
40	1.20	0.19	24.59	265	1.21	0.17	21.68
45	1.13	0.18	19.68	270	1.13	0.20	25.36
50	1.11	0.19	20.99	275	1.16	0.19	22.49
55	1.41	0.21	22.59	280	1.15	0.19	24.32
60	1.27	0.15	19.61	285	1.07	0.18	18.84
65	1.06	0.13	18.28	290	1.14	0.16	22.45
70	1.15	0.17	19.54	295	1.16	0.21	23.49
75	1.30	0.22	23.33	300	0.85	0.15	19.28
80	1.37	0.20	24.25	305	1.14	0.19	22.93
85	1.29	0.18	23.93	310	1.21	0.18	25.09
90	1.23	0.19	22.88	315	1.24	0.17	26.43
95	1.18	0.17	21.79	320	1.17	0.20	24.69
100	1.17	0.18	20.32	325	1.18	0.18	25.67
105	1.13	0.17	22.56	330	0.98	0.17	21.69
110	1.13	0.19	24.11	335	1.16	0.16	27.58
115	1.10	0.17	21.55	340	1.13	0.17	24.29
120	1.13	0.18	20.59	345	1.18	0.17	25.09
125	1.12	0.20	19.76	350	1.10	0.22	22.42
130	1.12	0.18	21.43	355	1.16	0.24	25.87
140	1.11	0.16	20.96	360	1.11	0.18	23.43
145	1.11	0.17	20.51	365	1.17	0.17	48.22
150	1.16	0.18	20.87	370	1.03	0.19	22.60
155	1.24	0.18	21.36	375	1.16	0.19	22.75
160	1.10	0.19	21.59	380	1.22	0.22	25.64
165	1.13	0.19	22.07	385	1.14	0.21	22.42
170	1.07	0.17	18.54	390	1.29	0.20	25.06
175	1.07	0.16	20.27	395	1.13	0.19	24.45
180	1.05	0.17	20.58	400	1.09	0.20	24.60
185	1.09	0.17	19.41	405	1.10	0.20	24.76
190	1.05	0.16	21.79	410	1.12	0.20	25.71
195	1.13	0.17	24.99	415	1.12	0.21	23.07
200	1.11	0.16	23.57	420	1.15	0.20	22.28
205	1.20	0.17	24.87	425	1.13	0.19	23.29
210	1.16	0.20	22.53	430	1.14	0.20	23.23
215	1.15	0.18	23.51	435	1.18	0.18	23.70
220	1.18	0.18	24.23	440	1.16	0.21	21.82
				443	1.08	0.18	22.96

sediments suggest that bloom conditions have occurred repeatedly. The abundance patterns of *Chaetoceros* RS in cores Gebra-1 and Gebra-2 agree with the high productivity values previously reported in Bransfield Basin (Wefer *et al.* 1988, Abelmann & Gersonde 1991, Bodungen *et al.* 1986). During much of the time represented, surface productivity in Bransfield Basin seems to have been much higher than today. The general trend is a progressive decrease in abundance towards the present (Fig. 7). Scherer & Leventer (1995) observed a similar pattern in *Chaetoceros* RS abundance, which they interpreted as a reduction in primary productivity from the last several thousand years to the present.

Another important component of the diatom assemblage is

comprised of the sea-ice taxa, used as a tracer of sea-ice extent by Gersonde (1986) and Gersonde *et al.* (1992). Zielinski & Gersonde (1997) reported a coincidence between the winter sea-ice extent in the Weddell and Scotia Seas and the northern boundary of significant occurrences of sea-ice taxa in surface sediments. This distribution was observed in the open ocean as well as in neritic environments such as those around northern Antarctic Peninsula. Abelmann & Gersonde (1991) observed in Bransfield Strait that during periods of sea-ice cover the vertical flux of biosiliceous particles was very low, and that maximum values of sea-ice taxa are reached during and after ice retreat. Intervals of increased sea-ice taxa in cores Gebra-1 and Gebra-2 suggest more extensive sea-ice

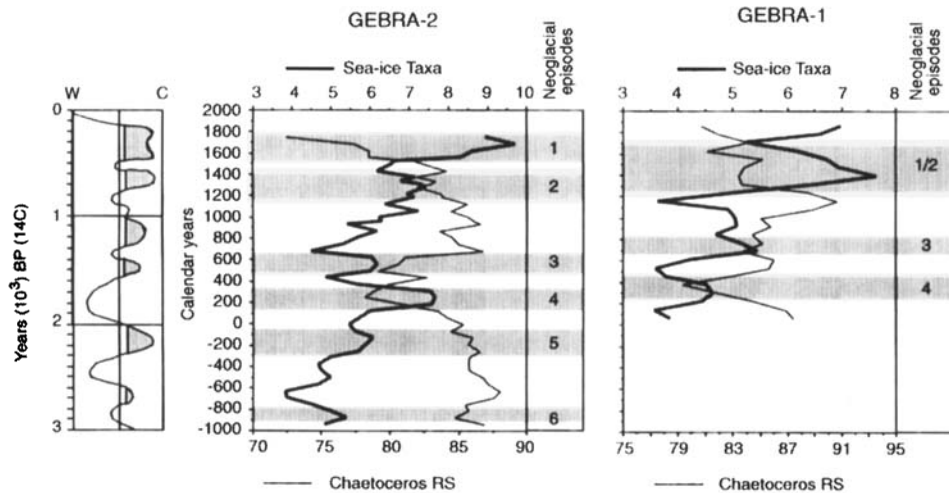


Fig 7. Record of neogacial events for the last three millennia after Wigley & Kelly (1990; box at left) vs Gebra-1 and Gebra-2 diatom variations. W and C refers to warm (glaciers less advanced) and cold (glaciers more advanced). Neogacial events labelled 1 to 6 and marked with grey horizontal bars. Maximum values of sea-ice taxa correspond to neogacial events.

cover, both spatially and seasonally (Fig. 7). Inter-neogacial periods were characterized by increases in *Chaetoceros* RS and by decreases in sea-ice taxa. Warmer temperatures and shorter sea-ice coverage periods would have been re-established in Bransfield Basin and the palaeoceanographic regime might have been similar to that observed today. The progressive increase in sea-ice taxa for the last three millennia seems to indicate a cooling trend. A similar pattern was observed by Leventer *et al.* (1996).

Thalassiosira antarctica/*T. scotia* RS are open-ocean forms which are more abundant in the Weddell and Scotia seas than in the Bransfield Strait area, although they have been reported frequently in both sediment traps and in surface sediments of the Bransfield Basin (Bodungen *et al.* 1986, Gersonde & Wefer 1987, Klöser 1990, Wefer *et al.* 1990, Abelmann & Gersonde 1991, Bárcena & Flores 1991, Zielinski 1993, Zielinski & Gersonde 1997). Significant changes in *T. antarctica*/*T. scotia* RS abundance may be related to oceanographic changes, in particular to the entrance of cold waters from the western Weddell Sea into Bransfield Strait (Eisele *et al.* 1986). Whereas in Bransfield Strait area neogacial episodes would have been characterized by shorter summers with sea-ice retreat, the western Weddell Sea would have been covered by sea-ice even during the summer. This would have prevented the development of *T. antarctica*/*T. scotia* RS since they require open water areas, and hence the supply of *T. antarctica*/*T. scotia* RS into Bransfield Basin would have been severely reduced.

Fragilariopsis kerguelensis, a characteristic species of the Antarctic Circumpolar Current (ACC) (Fenner *et al.* 1976, Burckle 1984, 1987), is common in surface sediments of the Southern Ocean (Zielinski 1993, Zielinski & Gersonde 1997). It dominates the sediment trap assemblages and surface sediments of Drake Passage (Gersonde & Wefer 1987, Leventer 1991, Abelmann & Gersonde 1991) but forms less than 2.5% of the assemblage in Bransfield Basin. In the planktonic assemblage, Nöthig (1988) reported a preferential

distribution of *F. kerguelensis* outside of Bransfield Basin. For these reasons, Leventer (1991) related the distribution of *F. kerguelensis* in Bransfield Basin to the incoming of water from the west (either the Bellingshausen Sea, or the ACC), using its abundance pattern to trace surface water currents. In Gebra-2 and Gebra-1, the abundance of this taxon is lower where sea-ice taxa reach their maxima. *Fragilariopsis kerguelensis* shows parallel shifts in abundance (but of lower amplitude) to those shown by *T. antarctica*/*T. scotia* RS (Fig. 8). Therefore, these two diatom groups, *T. antarctica*/*T. scotia* RS and *F. kerguelensis*, may be used to delineate oceanographic changes in Bransfield Basin.

Significance of radiolarians in Bransfield Basin

As seen for the diatoms, the annual radiolarian flux in settling assemblages occurs over a short time interval during the summer, when open-water conditions prevail. This flux is therefore strongly controlled by the sea-ice cover (Abelmann 1992a). According to that author, the *Phormacantha*/*Plectacantha* group is the main component of the coastal assemblage, preferring a neritic cold water habitat. In sediment traps located south of King George Island, Abelmann (1992a) documented a significant increase in this group, together with an increase in lithogenic components, towards the deeper part of the water column. This observation allowed him to relate the presence of the group in Bransfield Basin to lateral transport by turbidity currents from fjords and a rough continental shelf. From our observations, the maximum abundances of this group in the two Gebra cores would characterize oceanographic conditions similar to those observed today.

In the Bransfield Basin area, the *Lithomelissa* group is the main constituent of the pelagic assemblages while typical circumpolar species from the genus *Antarctissa* are rare. Abelmann (1992a) related the *Lithomelissa* group to the entrance of cold waters from the western Weddell Sea into

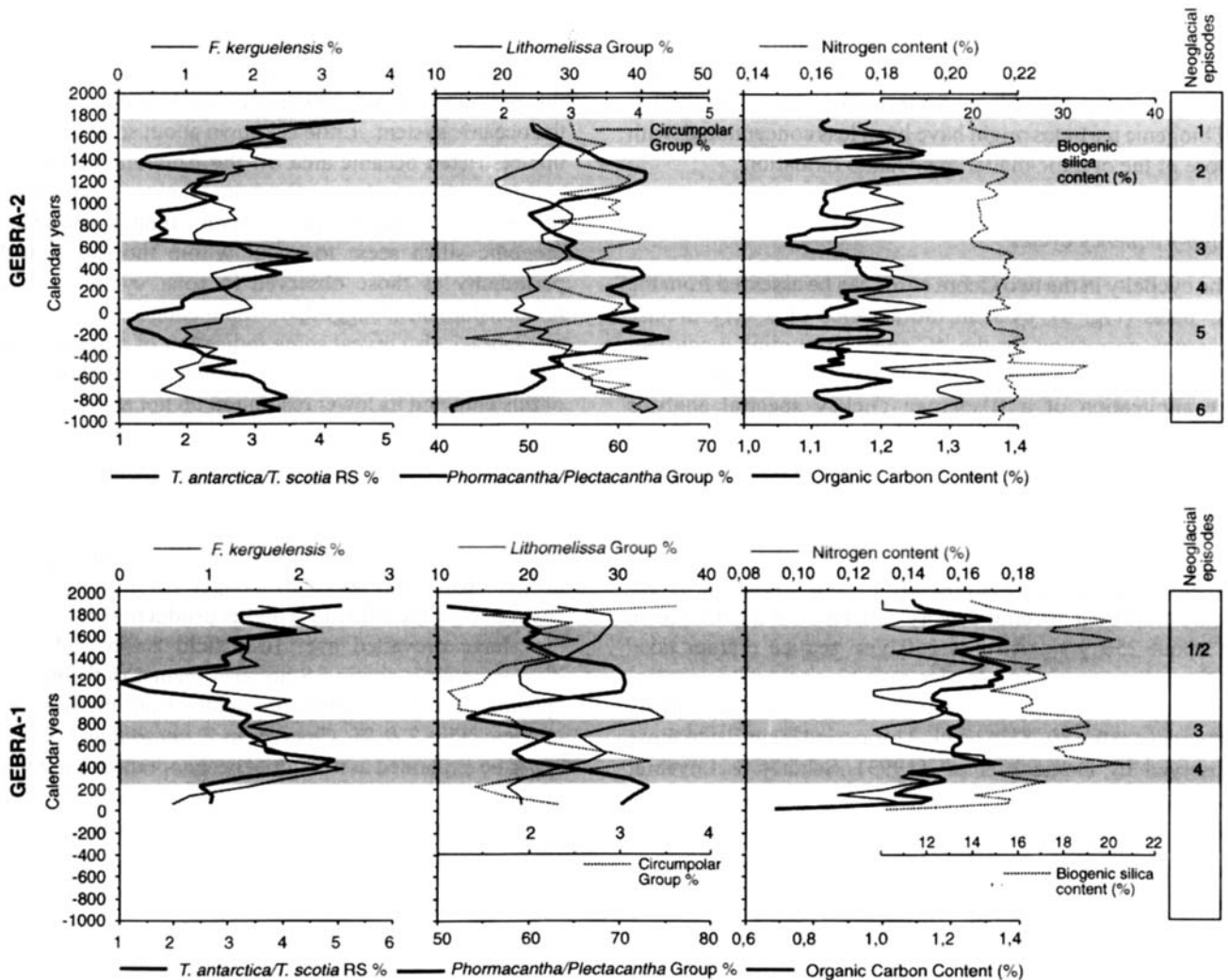


Fig 8. Diatom and radiolarian abundance patterns, with geochemical data and their relationship to the Holocene neoglacial episodes.

Maxima for the "circumpolar" radiolarian group occur during the interneoglacial events, while maxima in TOC, nitrogen and biogenic silica occur mainly during the neoglacial episodes.

Bransfield Strait. Therefore, low amounts of circumpolar species may characterize the normally restricted oceanographic conditions of Bransfield Basin, while higher values for the *Lithomelissa* group would suggest the entrance of cold water from the Weddell Sea. We consider the circumpolar group (composed by *A. denticulata* and *L. buetschlii*) to indicate the entrance of warmer waters from the ACC and/or the Bellingshausen Sea. Thus, increases in this group reflect input of warmer waters from the west. The opposite behaviour of the circumpolar group and of the sea-ice diatom taxa also suggests a restricted communication between the Bransfield Basin and the ACC. During maximum sea-ice extension, a reduced number of radiolarians from other basins entered Bransfield Basin (Fig. 8).

Sediment geochemistry

Values for biogenic silica, nitrogen and TOC are of the same order of magnitude as those recorded in the literature

(Figs 6 & 8; Yoon *et al.* 1994, Leventer *et al.* 1996). Leventer *et al.* (1996) observed that higher TOC is associated with drops in magnetic susceptibility, and related this to warmer climatic conditions. In the present study, maxima in TOC and nitrogen content are mainly related to the neoglacial events, in contradiction to the pattern observed by Leventer *et al.* (1996; Fig. 8). According to Yoon *et al.* (1994) high TOC in Bransfield Strait sediments is associated with increased palaeoproductivity in surface water rather than with an anoxic depositional environment. Jordan & Pudsey (1992) and Leventer *et al.* (1996) postulated that close to the receding ice edges, as a result of the sea ice melting and increased upper water column stratification, high planktonic cell density occurs. Under these conditions, the large amount of biogenic material produced flocculates and descends rapidly as aggregates to the seafloor, preventing organic matter dissolution. A similar situation is thought to have occurred for Gebra-1 and Gebra-2; a high amount of biogenic particles produced and precipitated during the sea-ice melting would

preserve the organic matter at the sea floor during neoglacial stages. Although during inter-neoglacial episodes surface productivity could be higher for the entire season, the settling of biogenic particles might have been less concentrated, with more of the organic matter exposed to oxidation.

High-frequency cycles

The cyclicity in the two Gebra cores can be assessed from the ^{14}C dates (Fig. 3), even in the absence of a very precise reservoir correction for the ^{14}C ages. Assuming a constant sedimentation rate between each age control point of Gebra-2, the application of a Blackman-Tuckey spectral analysis routines (Analyses series 1.1, Paillard *et al.* 1996) on different diatom and radiolarian taxa and on TOC%, N% and biogenic silica contents results in a dominant periodicity of 230 yrs, using a Bartlett Window type, a confidence interval of 80% and a band width of 0.0175 (Fig. 9). A cross spectral analysis of the *T. antarctica*/*T. scotia* group and *Chaetoceros* RS demonstrate their spectral density coherence at the 95% level at about 250 yrs. Also at 250 yrs, sea-ice diatom taxa/*Lithomelissa* group and sea-ice taxa/biogenic silica content cross spectral analyses produce good spectral density coherence at the 80–85% level. This period is similar to those observed by Domack *et al.* (1993), Scherer & Leventer (1995) and Leventer *et al.* (1996). The regional reservoir effect, as well as local processes, have a strong influence on

stratigraphic age control, and therefore the cyclicity period could undergo some variations. Leventer *et al.* (1996) related this periodicity to the 200 yr solar cycle and its influence on the oceanic system. Little is known about solar influence on this restricted oceanic area off the Antarctic continent, but since the observed variations in planktonic communities (diatoms and radiolarians), organic matter, nitrogen and biogenic silica seem to occur within the same range of periodicity as those observed in solar cycles, a possible relationship can be suggested. Application of spectral analyses on Gebra-1 also reveal some indication of a high frequency cyclicity at about 200–300 yrs. However, the shorter length of this core and its lower resolution do not provide results as good as those from Gebra-2.

Palaeoceanographic and palaeoclimatic changes

A relative increase in sea-ice taxa is observed during Holocene neoglacial events (Figs 7 & 8). Longer, but still not permanent, sea-ice coverage inducing a higher production of sea-ice taxa may have prevailed over Bransfield Basin. Maxima in *T. antarctica*/*T. scotia* RS are also related to the neoglacial episodes, but at different core depths from the sea-ice taxa maxima (Figs 7 & 8). Changes in *T. antarctica*/*T. scotia* RS could be explained as a result of oceanographic conditions in the Weddell Sea. During the neoglacial events, the western Weddell Sea would have remained ice-covered for longer

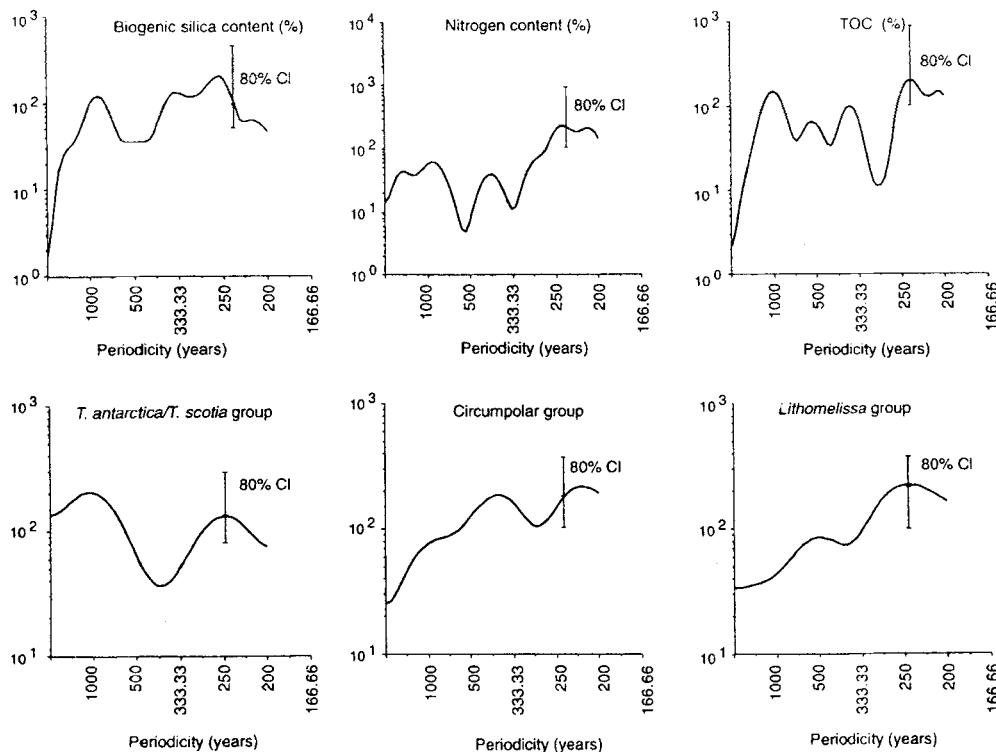


Fig 9. Spectral analysis of different parameters calculated for core Gebra-2. The signal has a statistically significant (80% level) concentration of the variance at the ≈ 230 yr periodicity. The x-axis shows periodicity in years. The y-axis shows spectral density (logarithmic scale).

during the summer. Thus, it is possible that the winter restriction between the Weddell Sea and the Bransfield Basin would have continued during the summer. This would have severely reduced the numbers of *T. antarctica*/*T. scotia* RS.

Warming would have resulted in a shorter seasonal duration of sea-ice cover in the Bransfield Strait and therefore the abundance of sea-ice taxa would have been reduced. In the western Weddell Sea, sea ice would have retreated during the summers, allowing the development of *T. antarctica*/*T. scotia* RS. Summer exchange between the Weddell Sea and the Bransfield Basin would have been re-established for longer time spans and a higher amount of *T. antarctica*/*T. scotia* RS could have entered the Bransfield Basin. A similar palaeoceanographic pattern is delineated by the *Lithomelissa* group. The abundance pattern of this group is in general the inverse of that of the sea-ice taxa (Figs 7 & 8). Thus, the higher values in the *Lithomelissa* group occurring during the interneoglacial periods could be related to the entrance of cold water from the Weddell Sea, once the Bransfield/Weddell communication had been re-established.

An equivalent situation may have occurred in the western Bransfield sub-basin regarding communication with the Bellingshausen Sea and the ACC. Slight increases in the abundance of *F. kerguelensis* during the terminal period of each neoglacial event may be related to the opening of this communication. Larger areas of open water may have allowed this species to flourish during the last stage of the neoglacial events. Therefore, during the terminal phases the east-flowing surface current entering the Bransfield Basin would have brought in *F. kerguelensis*. This interpretation is also supported by the distribution of radiolarians. The opposite trend of the radiolarian "circumpolar" group and the sea-ice taxa also points to a restricted communication between the Bransfield Basin and the ACC. During the maximum sea-ice extent, only a reduced number of allochthonous radiolarians entered the Bransfield Basin (Fig. 8). Since interneoglacial periods are characterized by increases in *Chaetoceros* RS, the *Lithomelissa* group and the "circumpolar group", and by decreases in sea-ice taxa, *T. antarctica*/*T. scotia* RS and *F. kerguelensis* the palaeoceanographic regime at these times might have been similar to that existing today.

Conclusions

The AMS ¹⁴C chronology yielded for core tops an older age than expected for cores Gebra-1 and Gebra-2: 2985 ± 39 yr BP and 2796 ± 34 yr BP respectively. ²¹⁰Pb γ-spectrometry places the core top of Gebra-1 within the last sixty years. The sedimentation rate calculated for Gebra-1 is 130 cm kyr⁻¹, and for Gebra-2 160 cm kyr⁻¹.

The variations in the siliceous fossil assemblages recorded in Gebra-1 and Gebra-2 correspond to the neoglacial events known for the Holocene. Changes in species composition reflect changes in environmental conditions, including water masses and sea-ice cover. Diatoms and radiolarians have

been used to delineate variations in water masses. *T. antarctica*/*T. scotia* RS and the *Lithomelissa* group are related to the cold water from the western Weddell Sea. *Fragilariopsis kerguelensis* and the circumpolar group are related to the ACC and waters from the Bellingshausen Sea.

The abundance patterns of *Chaetoceros* RS in cores Gebra-1 and Gebra-2 agree with the high productivity values reported for the Bransfield Basin waters. Past surface productivity in the Bransfield Basin was higher than today. The general trend indicates a reduction in palaeoproductivity. Besides, the progressive increase in sea-ice taxa for the last three millennia seems to indicate a cooling trend.

Based on the distribution of siliceous microfossils, two climatic and palaeoceanographic scenarios have been described: Neoglacial episodes characterized by greater and longer sea-ice coverage and a restricted Weddell/Bransfield/Bellingshausen summer communication. A climatic amelioration could have restored the Weddell/Bransfield/Bellingshausen communication during summers. The interneoglacial phases were characterized by a palaeoclimatic and palaeoceanographic regime similar to that observed today. These changes have an overprinted high frequency cyclicity at about 200–300 yr, which might be related to the 200 yr solar cycle.

Acknowledgements

Funding for this work was generously supported by the Spanish CICYT projects ANT93-1008-CO301, ANT93-1008-CO203, ANT94-0277 and PB95-0927-CO2-01, and by Deutsche Forschungsgemeinschaft (Ge 516/5). This is Alfred Wegener Institute contribution no. 1442.

The authors would like to thank N. Skinner for revising the English version of the manuscript and J. Roncero for technical assistance. We also thank Dr Amy Leventer and Dr John Barron for reviewing the manuscript.

References

- ABELMANN, A., BOCK, U., GERSONDE, R. & TREPPKE, U.F. in press. A revised preparation technique for siliceous microfossils. *Micropaleontology*.
- ABELMANN, A. 1992a. Radiolarian flux in Antarctic waters (Drake Passage, Powell Basin, Bransfield Strait). *Polar Biology*, **12**, 357-372.
- ABELMANN, A. 1992b. Radiolarian taxa from Southern Ocean sediment traps (Atlantic Sector). *Polar Biology*, **12**, 373-385.
- ABELMANN, A. & GERSONDE, R. 1991. Biosiliceous particle flux in the Southern Ocean. *Marine Chemistry*, **35**, 503-536.
- AMOS, A.F. 1987. RACER: physical oceanography of the western Bransfield Strait. *Antarctic Journal of the United States*, **22**(5), 137-140.
- BÁRCENA, M.A. & FLORES, J.A. 1991. Distribución y microtafonomía de las asociaciones de diatomeas de sedimentos superficiales en el sector Atlántico del Océano Antártico. *Revista Española de Paleontología*, **5**, 53-6.

- BAREILLE, G., LABRACHERIE, M., LABEYRIE, L., PICHON, J.J. & TURON, J.L. 1991. Biogenic silica accumulation rate during the Holocene in the south-eastern Indian Ocean. *Marine Chemistry*, **35**, 537-551.
- BARNOLA, J.M., ANKLIN, M., PORCHERON, J., RAYNAUD, D., SCHWANDER, J. & STAUFFER, B. 1995. CO₂ evolution during the last millennium as recorded by Antarctic and Greenland ice. *Tellus*, **47B**, 264-272.
- BARTSCH, A. 1989. Die Eisalgenflora des Weddellmeeres (Antarktis): Artenzusammen-setzung und biomasse sowie Ökophysiologie ausgewählter Arten. *Berichte zur Polarforschung*, **63**, 1-110.
- BERKMAN, P.A., ANDREWS, J.T., BJÖRK, S., *et al.* 1998. Circum-Antarctic coastal environmental shifts during the Late Quaternary reflected by emerged marine deposits. *Antarctic Science*, **10**, 345-362.
- BIRKENMAJER, K. 1992. Cenozoic glacial history of the South Shetlands and northern Antarctic Peninsula. In LOPEZ-MARTINEZ, J., ed. *Geología de la Antártida Occidental*, III Congreso Geológico de España y VIII Congreso Latinoamericano de Geología, Salamanca. *Simpósios*, **3**, 251-260.
- BJÖRCK, S., OLSSON, S., ELLIS-EVANS, C., HÅKANSSON, H., HUMLUM, O. & DE LIRIO, J.M. 1996. Late Holocene palaeoclimate records from lake sediments on James Ross Island, Antarctica. *Palaeogeography, Palaeoclimatology, Palaeoecology*, **121**, 195-220.
- BODUGEN, B., SMETACEK, V.S., TILZER, M.M. & ZEITSCHEL, B. 1986. Primary productivity and sedimentation during spring in the Antarctic Peninsula region. *Deep-Sea Research*, **33**, 177-194.
- BURCKLE, L.H. 1984. Ecology and Paleocology of the marine diatom *Eucampia antarctica* (Castr.) Mangin. *Marine Micropaleontology*, **9**, 77-86.
- BURCKLE, L.H. 1987. Diatom distribution in the Weddell Gyre region during the late winter. *Micropaleontology*, **33**, 177-184.
- BURCKLE, L.H. & BURAK, R.W. 1988. Fluctuations in late Quaternary diatom abundances: stratigraphic and paleoclimatic implications from subantarctic deep sea cores. *Palaeogeography, Palaeoclimatology, Palaeoecology*, **67**, 147-156.
- BURCKLE, L.H. & COOKE, D.W. 1983. Late Pleistocene *Eucampia antarctica* abundance stratigraphy in the Atlantic sector of the Southern Ocean. *Micropaleontology*, **29**, 6-10.
- CANALS, M. & GEBRAP'96 TEAM. 1997. Evolución geológica del margen pacífico de la Antártida Occidental: Expansion del fondo oceánico y tectónica de placas. *Informe final de la Campana GEBRAP '96*, 187 pp. [Internal report].
- DEMASTER, D.J., NELSON, T.M., NITTROUER, C.A. & HARDEN, S.L. 1987. Biogenic silica and organic carbon accumulation in modern Bransfield Strait sediments. *Antarctic Journal of the United States*, **22**(5), 108-110.
- DOMACK, E.W., MASHIOTTA, T.A. & BURKLEY, L.A. 1993. 300-year cyclicity in organic matter preservation in Antarctic fjord sediments. *Antarctic Research Series*, **60**, 265-271.
- EISELE, R., WITTHINRICH, J. & WITTSTOCK, R.-R. 1986. Ozeanographische Untersuchungen. In FÜTTERER, D., ed. *Die Expedition ANTARKTIS-IV mit FS-Polarstern 1985/86*. *Berichte zur Polarforschung*, **32**, 86-87.
- ERCILLA, G., BARAZA, J., ALONSO, B. & CANALS, M. 1997. Recent geological processes in the Central Bransfield Basin (Western Antarctic Peninsula). In STOKER, M.S., EVANS, D. & CRAMP, A., eds. *Geological processes on continental margins: sedimentation, mass-wasting and stability*. *Geological Society of London, Special Publication*, **129**, 205-216.
- FABRES, J., CALAFAT, A.M., CANALS, M., FRANCÉS, G., BÀRCENA, M.A., LEDESMA, S. & FLORES, J.A. 1997. Identificación de procesos sedimentarios en la Cuenca de Bransfield (Antártida Occidental). *Boletín de la Real Sociedad Española de Historia Natural*, **93**, 85-94.
- FENNER, J., SCHRADER, H.J. & WEINIG, H. 1976. Diatom phytoplankton studies in the Southern Pacific Ocean, composition and correlation to the Antarctic Convergence and its paleoecological significance. *Initial Reports of the Deep Sea Drilling Project*, **35**, 757-813.
- FRYXELL, G.A., REAP, M.E. & KANG, S.H. 1988. Antarctic phytoplankton-dominants, life stages, and indicators. *Antarctic Journal of the United States*, **25**(3), 129-131.
- GARCIA-CORDON, J.C. 1996. Un clima para la historia: una historia para el clima. *Lecciones 2/96*, Universidad de Cantabria, 95 pp.
- GERSONDE, R. 1986. Siliceous microorganisms in sea ice and their record in sediments in the southern Weddell Sea (Antarctica). *Proceedings of the VIIIth Symposium on Living and Fossil Diatoms*, 549-566.
- GERSONDE, R. & WEFER, G. 1987. Sedimentation of biogenic siliceous particles in Antarctic waters from the Atlantic sector. *Marine Micropaleontology*, **11**, 311-332.
- GORDON, A.L. & NOWLIN, W.D. 1978. The basin waters of the Bransfield Strait. *Journal of Physical Oceanography*, **8**, 258-264.
- GRACIA, E., CANALS, M., FARRAN, M., ACOSTA, J., PRIETO, M.J. & GEBRA TEAM. 1995. The Bransfield backarc basin (NW Antarctic Peninsula): the initial stage of seafloor spreading. *VII International Symposium on Antarctic Earth Sciences (ISAES)*, 10-15 September, Siena, Italy, 165-166.
- FARRAN, M., ACOSTA, J., PRIETO, M.J. & GEBRA TEAM. 1996. Morphostructure and evolution of the Bransfield back-arc basin (NW Antarctic Peninsula). *Marine Geophysical Researches*, **18**, 429-448.
- GROVE, J.M. 1988. *The Little Ice Age*. Cambridge: Cambridge University Press, 498 pp.
- HARDEN, S.L., DEMASTER, D.J. & NITTROUER, C.A. 1992. Developing sediment geochronologies for high-latitude continental shelf deposits: a radiochemical approach. *Marine Geology*, **103**, 69-97.
- HARGRAVES, P.E. 1968. *Species composition and distribution of the net plankton diatoms in the Pacific sector of the Antarctic Ocean*. Ph.D. thesis, College of William and Mary, Virginia, 171 pp. [unpublished].
- HASLE, G.R. 1965. *Nitzschia* and *Fragilariopsis* species studied in the light and electron microscopes. III. The genus *Fragilariopsis*. *Skriptor Utgitt av det Norske Videnskaps-Akademi i Oslo Mat.-Naturv. Klasse, Ny Serie*, no. 21.
- HASLE, G.R. 1969. An analysis of the phytoplankton of the Pacific Southern Ocean: Abundance, composition, and distribution during the Bratigg expedition, 1947-1948. *Hvalrådets skriffter*, **52**, 1-168.
- HEIDEN, H. & KOLBE, R.W. 1928. Die marinen Diatomeen der Deutsch Südpolar-Expedition 1901-1903. *Deutsch Südpolar-Expedition 1901-1903*, **8**, 450-714.
- INGÖLFSSON, Ö., HJORT, C., BERKMAN, P.A., BJÖRK, COLHOUN, E., GOODWIN, I.D., HALL, B., HIRAKAWA, K., MELLES, M., MÖLLER, P. & PRENTICE, M.L. 1998. Antarctic glacial history since the Last Glacial Maximum: an overview of the record on land. *Antarctic Science*, **10**, 326-345.
- JEFFERS, J.D. 1988. *Tectonic and sedimentary evolution of the Bransfield Basin, Antarctica*. Ph.D. dissertation, Rice University, Houston, 142 pp. [unpublished].
- JEFFERS, J.D. & ANDERSON, J.B. 1990. Sequence stratigraphy of the Bransfield Basin, Antarctica: implications for tectonic history and hydrocarbon potential. In JOHN, B.S., eds. *Antarctica as an exploration frontier-hydrocarbon potential, geology, and hazards*. AAPG Studies in Geology, **31**, 13-29.
- JORDAN, R.W. & PUDSEY, C.J. 1992. High-resolution diatom stratigraphy of Quaternary sediments from the Scotia Sea. *Marine Micropaleontology*, **19**, 201-237.
- KARSTEN, G. 1905-07. Das Phytoplankton des Antarktischen Meeres. In CHUN, C., ed. *Wissenschaftliche Ergebnisse der deutschen Tiefsee-Expedition auf dem Dampfer "Valdivia", 1898-1899*. Jena: Fischer, 1-126.

- KELLOGG, D.A. & KELLOGG, T.B. 1987. Microfossil distributions in modern Amundsen Sea sediments. *Marine Micropaleontology*, **12**, 203-222.
- KIM, W.H. & PARK, B.K. 1988. Marine diatoms from the Quaternary sediments in the Marian Cove, King George Island, Antarctica. *Journal of the Paleontological Society of Korea*, **4**, 135-159.
- KLÖSER, H. 1990. Distribution of microplankton organisms north and west of the Antarctic Peninsula according to changing ecological conditions in autumn. *Berichte zur Polarforschung*, **77**, 1-255.
- KOZLOVA, O.G. 1966. *Diatoms of the Indian and Pacific Sectors of the Antarctic*. Jerusalem: Israel Program for Scientific Translations, 191 pp.
- KREBS, W.N. 1983. Ecology of neritic marine diatoms, Arthur Harbour, Antarctica. *Micropaleontology*, **29**, 267-297.
- LABAN, C. & DER VAN GROOT, T. 1986. A preliminary interpretation of the gravity cores. *Berichte zur Polarforschung*, **32**, 96-98.
- LAMB, H.H. 1965. The early medieval warm epoch and its sequel. *Palaeogeography, Palaeoclimatology, Palaeoecology*, **1**, 13-37.
- LEVENTER, A. 1991. Sediment trap diatom assemblages from the northern Antarctic Peninsula region. *Deep-Sea Research*, **38**, 1127-1143.
- LEVENTER, A., DOMACK, E., ISHMAN, S.E., BRACHFELD, S., MCCLENNEN, C.E. & MANLEY, P. 1996. Productivity cycles of 200-300 years in the Antarctic Peninsula region: Understanding linkages among the sun, atmosphere, oceans, sea ice, and biota. *Geological Society of America Bulletin*, **108**, 1626-1644.
- LEVENTER, A. & DUNBAR, R.B. 1988. Recent diatom record of McMurdo Sound, Antarctica: implications for history of sea ice extent. *Paleoceanography*, **3**, 259-274.
- MOLINA-CRUZ, A. 1977. Radiolarian assemblages and their relationship to the oceanography of the subtropical south-eastern Pacific. *Marine Micropaleontology*, **2**, 315-352.
- MÖRNER, N.A. 1984. Climatic changes on a yearly to millennial basis. Concluding remarks. In KARLÉN, W. & MÖRNER, N.A., eds. *Climatic changes on a yearly to millennial basis*. Dordrecht:Reidel, 637-651.
- MORTLOCK, R.A. & FROELICH, P.N. 1989. A simple method for the rapid determination of biogenic opal in pelagic marine sediments. *Deep-Sea Research*, **36**, 1415-1426.
- NAVAL OCEANOGRAPHY COMMAND DETACHMENT. 1985. *Sea ice climatic atlas: Volume I Antarctic*. Oceanographic Office, Dept of Navy, NAVAIR 50-1C-540. 132 pp.
- NÓTHIG, E.-V. 1988. On the ecology of the phytoplankton in the south-eastern Weddell Sea (Antarctica) in January/February 1985. *Berichte zur Polarforschung*, **53**, 118 pp.
- PAILLARD, D., LABEYRIE, L. & YIOU, P. 1996. Macintosh program performs time-series analyses. *Eos Trans.*, **77**, 379
- PRIESTLEY, M.B. 1981. *Spectral analysis of time series, vol. 1*. London: Academic Press, 653 pp.
- PRIETO, M.J. 1996. *Estratigrafía sísmica y evolución geodinámica de la Cuenca Central de Bransfield (Antártida Occidental)*. Tesis de Licenciatura, Universidad de Barcelona, 150 pp.
- PRIETO, M.J., CANALS, M., ERCILLA, G. & DE BATIST, M. in press a. Seismic stratigraphy of the Central Bransfield Basin (NW Antarctic Peninsula): interpretation of deposits and sedimentary processes in a glacio-marine environment. *Marine Geology*.
- PRIETO, M.J., CANALS, M., ERCILLA, G. & DE BATIST, M. in press b. Structure and geodynamic evolution of Central Bransfield Basin (NW Antarctica) from seismic reflection data. *Marine Geology*.
- SANFILIPPO, A., WESTBERG-SMITH, M.J. & RIEDEL, W.R. 1985. Cenozoic radiolaria. In BOLLI, H.M., SAUNDERS, J.B. & PERCH-NIELSEN, K., eds. *Plankton stratigraphy*. Cambridge: Cambridge University Press, Earth Science Series, 631-712.
- SCHAREK, R. 1991. Development of phytoplankton during the late-winter/spring transition in the eastern Weddell Sea (Antarctica). *Berichte zur Polarforschung*, **94**, 1-195.
- SCHERER, R. & LEVENTER, A. 1995. Holocene diatom productivity along the northern Antarctic Peninsula (Abstract). *Fifth International Conference on Paleoceanography*, Halifax, Canada, 171.
- SCHRADER, H.J. & GERSONDE, R. 1978. Diatoms and silicoflagellates. In ZACHARIASSE, W.J. et al., eds. *Micropaleontological counting methods and techniques- an exercise on an eight metres section of the lower Pliocene of Capo Rossello, Sicily*. *Utrecht Micropaleontological Bulletins*, **17**, 129-176.
- SINGER, J.K. 1987. *Terrigenous, biogenic, and volcanoclastic sedimentation patterns of the Bransfield Strait and bays of the northern Antarctic Peninsula: implications for Quaternary glacial history*. Ph.D. thesis, Rice University, Houston, 342 pp. [unpublished].
- STUIVER, M., DENTON, G.H., HUGHES, T.J. & FASTOOK, J.L. 1981. History of the marine ice sheet in west Antarctica during the last glaciation: a working hypothesis. In DENTON, G. & HUGHES, T., eds. *The Last Great Ice Sheets*. New York: John Wiley, 319-436.
- VAN ENST, J.W.A. 1987. ²¹⁰Pb activities in the Bransfield Strait, additional proof of hydrothermal activity (Abstract). *Fifth International Symposium on Antarctic Earth Sciences*, Cambridge, 166.
- VAN HEURCK, H. 1909. Diatomées. Expédition Antarctique Belge. *Resultats du Voyage de la "Belgica" en 1897-1899. Rapport Scientifiques. Botanique*, 128 pp.
- VENKATESAN, M.I. & KAPLAN, I.R. 1987. The lipid geochemistry of Antarctic marine sediments: Bransfield Strait. *Marine Chemistry*, **21**, 347-375.
- WEFER, G., FISCHER, G., FÜTTERER, D.K. & GERSONDE, R. 1988. Seasonal particle flux in the Bransfield Strait, Antarctica. *Deep-Sea Research*, **35**, 891-898.
- WEFER, G., FISCHER, G., FÜTTERER, D.K., GERSONDE, R., HONJO, S. & OSTERMANN, D. 1990. Particle sedimentation and productivity in Antarctic waters of the Atlantic Sector. In BLEIL, U. & THIEDE, J., eds. *Geologic history of the polar oceans: Arctic versus Antarctic*. NATO ASI Series C, **308**, Amsterdam: Kluwer, 363-379.
- WHITAKER, T.M. 1977. Sea ice habitats of Signy Island (South Orkneys) and their primary productivity. In LLANO, G.A., ed. *Adaptations within Antarctic ecosystems*. Washington, DC: Smithsonian Institution, 75-82.
- WIGLEY, T.M.L. & KELLY, P.M. 1990. Holocene climatic change, ¹⁴C wiggles and variations in solar irradiance. *Philosophical Transactions of the Royal Society of London*, **330**, 547-560.
- YOON, H.I., HAN, M.W., PARK, B.K., OH, J.K. & CHANG S.K. 1994. Depositional environment of near-surface sediments, King George Basin, Bransfield Strait, Antarctica. *Geo-Marine Letters*, **14**, 1-9.
- ZIELINSKI, U. 1993. Quantitative estimation of paleoenvironmental parameters of the Antarctic surface water in the Late Quaternary using transfer functions with diatoms. *Berichte zur Polarforschung*, **126**, 148 pp.
- ZIELINSKI, U. & GERSONDE, R. 1997. Diatom distribution in Southern Ocean surface sediments (Atlantic sector): implications for paleoenvironmental reconstructions. *Palaeogeography, Palaeoclimatology, Palaeoecology*, **129**, 213-250.